An Extract of Taro (*Colocasia esculenta*) Mediates Potent Inhibitory Actions on Metastatic and Cancer Stem Cells by Tumor Cell-Autonomous and Immune-Dependent Mechanisms

Namita Kundu[1,2], Xinrong Ma[2], Stephen Hoag[3] (iD), Fang Wang[3],
Ahmed Ibrahim[3] (iD), Raquel Godoy-Ruiz[2,4,5,6], David J Weber[2,4,5,6]
and Amy M Fulton[1,2,7] (iD)

[1]Department of Pathology, University of Maryland School of Medicine, Baltimore, MD, USA.
[2]University of Maryland Marlene and Stewart Greenebaum Comprehensive Cancer Center,
Baltimore, MD, USA. [3]University of Maryland School of Pharmacy, Baltimore, MD, USA.
[4]Department of Biochemistry and Molecular Biology, University of Maryland School of
Medicine, Baltimore, MD, USA. [5]Center for Biological Therapeutics (CBT), University of
Maryland School of Medicine, Baltimore, MD, USA. [6]Institute for Bioscience and Biotechnology
Research (IBBR), Rockville, MD, USA. [7]VA Administration Investigator, VA Health Services
Research and Development Service, Baltimore Veterans Administration Medical Center,
Baltimore, MD, USA.

ABSTRACT

The taro plant, *Colocasia esculenta*, contains bioactive proteins with potential as cancer therapeutics. Several groups have reported anticancer activity in vitro and in vivo of taro-derived extracts (TEs). We reported that TE inhibits metastasis in a syngeneic murine model of Triple-Negative Breast Cancer (TNBC).

PURPOSE: We sought to confirm our earlier studies in additional models and to identify novel mechanisms by which efficacy is achieved.

METHODS: We employed a panel of murine and human breast and ovarian cancer cell lines to determine the effect of TE on tumor cell viability, migration, and the ability to support cancer stem cells. Two syngeneic models of TNBC were employed to confirm our earlier report that TE potently inhibits metastasis. Cancer stem cell assays were employed to determine the ability of TE to inhibit tumorsphere-forming ability and to inhibit aldehyde dehydrogenase activity. To determine if host immunity contributes to the mechanism of metastasis inhibition, efficacy was assessed in immune-compromised mice.

RESULTS: We demonstrate that viability of some, but not all cell lines is inhibited by TE. Likewise, tumor cell migration is inhibited by TE. Using 2 immune competent, syngeneic models of TNBC, we confirm our earlier findings that tumor metastasis is potently inhibited by TE. We also demonstrate, for the first time, that TE directly inhibits breast cancer stem cells. Administration of TE to mice elicits expansion of several spleen cell populations but it was not known if host immune cells contribute to the mechanism by which TE inhibits tumor cell dissemination. In novel findings, we now show that the ability of TE to inhibit metastasis relies on immune T-cell-dependent, but not B cell or Natural Killer (NK)-cell-dependent mechanisms. Thus, both tumor cell-autonomous and host immune factors contribute to the mechanisms underlying TE efficacy. Our long-term goal is to evaluate TE efficacy in clinical trials. Most of our past studies as well as many of the results reported in this report were carried out using an isolation protocol described earlier (TE). In preparation for a near future clinical trial, we have now developed a strategy to isolate an enriched taro fraction, TE-method 2, (TE-M2) as well as a more purified subfraction (TE-M2F1) which can be scaled up under Good Manufacturing Practice (GMP) conditions for evaluation in human subjects. We demonstrate that TE-M2 and TE-M2F1 retain the anti-metastatic properties of TE.

CONCLUSIONS: These studies provide further support for the continued examination of biologically active components of *Colocasia esculenta* as potential new therapeutic entities and identify a method to isolate sufficient quantities under GMP conditions to conduct early phase clinical studies.

KEYWORDS: Taro, *Colocasia esculenta*, metastasis, cancer stem cell, immune-modulatory

Introduction

Tumor dissemination, and the establishment of metastatic lesions, is the major source of breast cancer mortality. Identification of therapeutic approaches to inhibit metastasis is an unrealized goal. Approximately 50% to 70% of US Food and Drug Administration (FDA)-approved cancer therapeutics are either natural products or natural product pharmacophores. Potential medicinal properties of the Taro corm, *Colocasia*

esculenta have been described for centuries.[1] Brown et al[2] first described potential anti-proliferative activity of taro-derived products on colon cancer cells in vitro. We have previously reported a potent anti-metastatic activity derived from a water-soluble extract of taro, taro extract (TE)[3] in 2 models of Triple-Negative Breast Cancer (TNBC). We now confirm, in the same models, that near total suppression of metastasis was achieved in immune competent mice treated with TE. The current studies were carried out to gain insights into the mechanisms of action by which TE inhibits metastasis and to identify a relevant way to isolate an active fraction that is more easily scaled up so that it could be produced under Good Manufacturing Practice (GMP) for future clinical evaluation. Both tumor cell-autonomous and indirect effects of TE on the host immune response were explored. Using an expanded panel of human breast cancer cell lines, as well as ovarian cancer cell lines, we first confirmed the ability of TE to directly inhibit the migration and proliferation of tumor cells in vitro. We also investigated, for the first time, the ability of TE to inhibit properties of breast cancer stem cells (CSCs). Several groups have described expansion of hematopoietic cells including B lymphocytes in response to taro-derived proteins[4-8] but whether B cells, or other immune effector cells, contribute *mechanistically* to TE efficacy has not been reported. In the current study, we examine the potential contribution of immune effector cells to the therapeutic mechanism of TE. We reported previously that a subfraction of TE, obtained using size exclusion chromatography (SEC), amplified the potent anti-metastatic activity in TE. In anticipation of future phase I clinical trials, we sought a means to isolate this active fraction using methods that are scalable and adaptable to production under GMP conditions. We now report that isolation and preparation by a combination of ultrafiltration, SEC, and spray-drying processes provide the fully active component of TE, designated TE-method 2, Fraction 1 (TE-M2F1) in a scalable manner that retains the anti-metastatic activity of TE.

Materials and Methods

Ethics statement

All animal experiments were approved by the Institutional Animal Care and Use Committee (IACUC) of the University of Maryland School of Medicine and carried out in strict accordance with the recommendations in the guide for the Care and Use of Laboratory Animals of the National Institutes of Health (United States).

Mice

Syngeneic Balb/cByJ female mice were purchased from Jackson Laboratories (Bar Harbor, ME). Fox Chase severe combined immune deficient (SCID) female mice were purchased from Charles River (Newark, DE). All mice were housed in micro-isolator cages, fed conventional, autoclaved chow, and provided drinking water ad libitum.
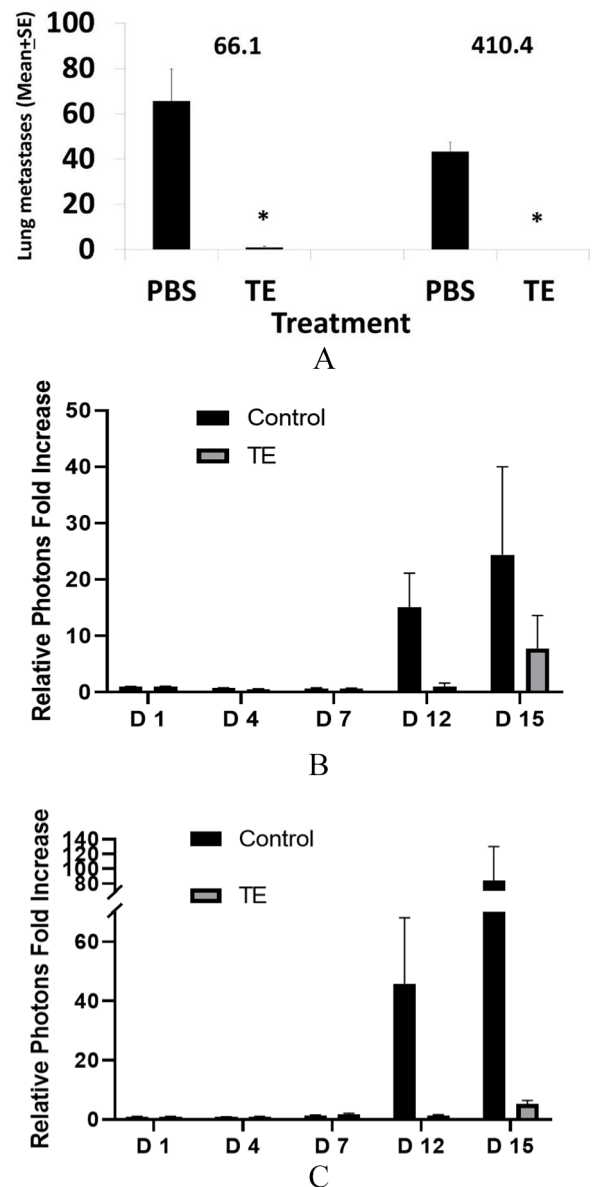

Figure 1. (A) Balb/cByJ female mice treated daily with TE (400 ug protein in 200 µL PBS) or PBS for 10 days. On day 4, mice were injected IV with either 2.0×10^5 of line 66.1 cells or 1.5×10^5 of line 410.4 cells. On day 17 (66.1) or day 19 (410.4) from tumor cell injections, mice were euthanized and surface lung tumor colonies enumerated. *$P < .0001$. (B, C) Mice injected with 2×10^5 66.1-luc cells and bioluminescent imaging conducted on days + 1, + 4, and + 15 relative to tumor cell injection. Photon increase relative to day 0 in (B) brain or (C) bone marrow, respectively. PBS indicates phosphate-buffered saline; TE, taro extract.

Taro extract preparation

Two extraction procedures were used for these studies. Method 1 was as described previously[3] and hereafter designated as TE. This method was employed in studies reported in Figures 1 to 7. Method 2 was carried out with minor modifications of Method 1 to confirm the earlier findings in an independent lab and to standardize early steps including peeling and homogenization of taro corms. The final goal was to isolate the active TE fraction, in a scalable method adaptable to GMP production, designated TE-M2. Commercially obtained Taro corm was
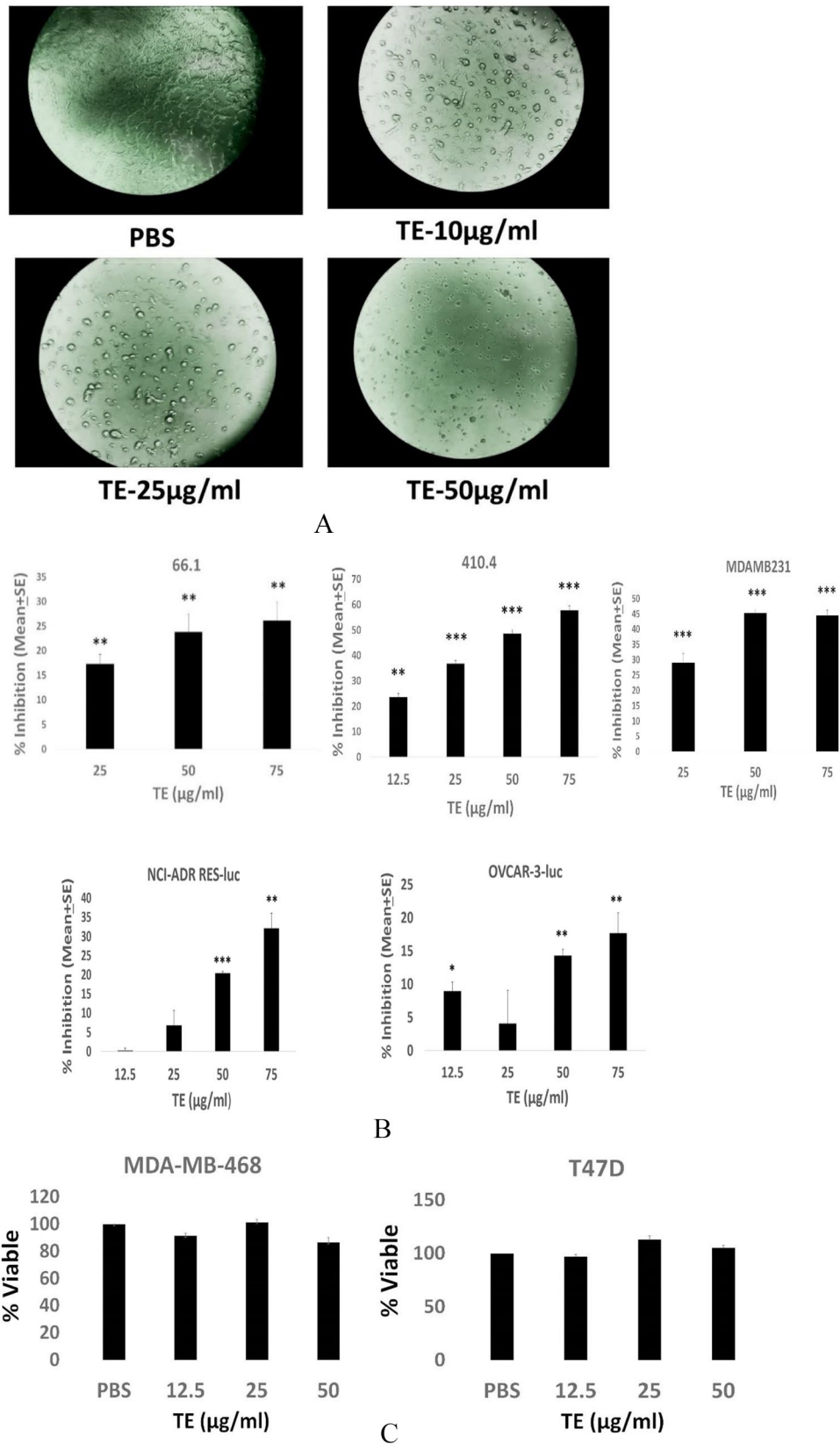
Figure 2. TE inhibits cell viability. (A) Appearance of 66.1 cells treated with PBS or TE at several concentrations. 40× magnification. (B, C) Murine (66.1, 410.4) or human (MDA-MD-231, MDA-MB-468, T47D) breast cancer cells or ovarian cancer cells (NCI-ADR RES-luc; OVCAR-3-luc) were seeded in triplicate and PBS or TE was added at final protein concentrations of 12.5, 25, 50, or 75 μg/mL. At 72 hours, cell viability was determined by MTT assay and expressed as % inhibition versus PBS-treated cells (B) *$P < .05$; ** $P < .002$; *** $P < .001$. In (C), data are plotted as % viable versus PBS-treated cells where PBS = 100% viable. No significant differences observed. PBS indicates phosphate-buffered saline; TE, taro extract.

Figure 3. Human (BT-549-GFP; MDA-MB-231) or murine (66.1; 410.4) cells placed in upper wells of migration chamber and allowed to migrate in response to 2% FBS in the absence or presence of TE in the upper and lower chamber, at the indicated concentrations or vehicle control for 18 to 20 hours. Cells in lower chamber stained with calcein AM, dislodged with colorless trypsin, and cell number estimate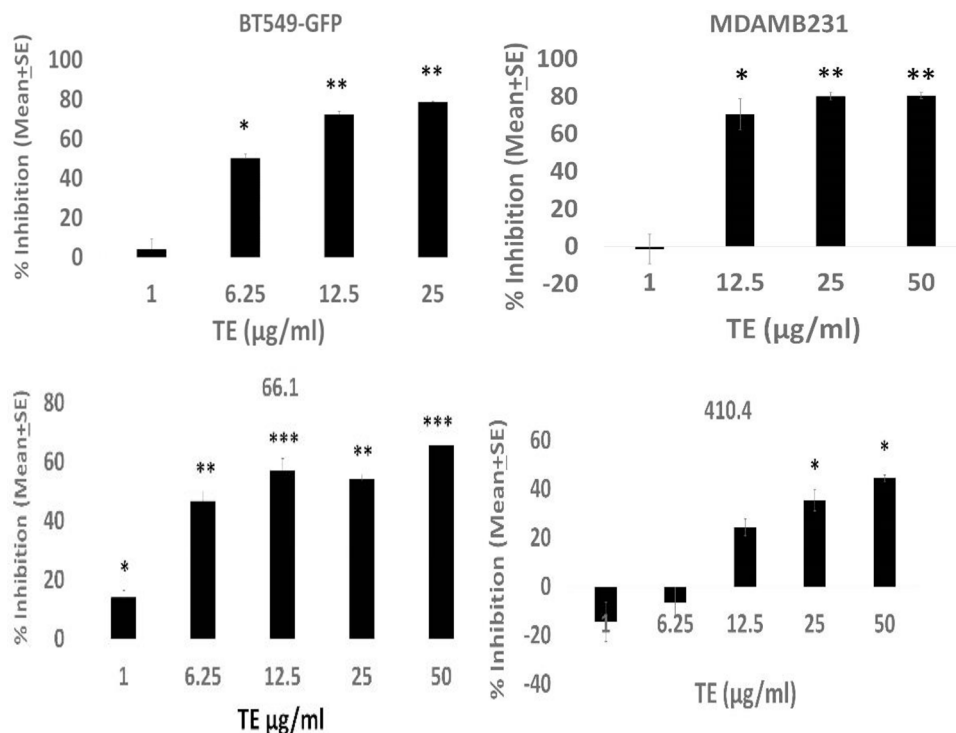d. Ex-485; Emi-520. Mean migration $\pm$ SE of triplicate determinations expressed as % inhibition versus PBS-treated cells. For BT549-GFP, 66.1, and 4104 cells, *P* values are *P < .04; **P < .003; ***P < .0006. For MDA-MB-231 cells, *P* values are *P < .04; **P < .02. FBS indicates fetal bovine serum; PBS, phosphate-buffered saline; TE, taro extract.
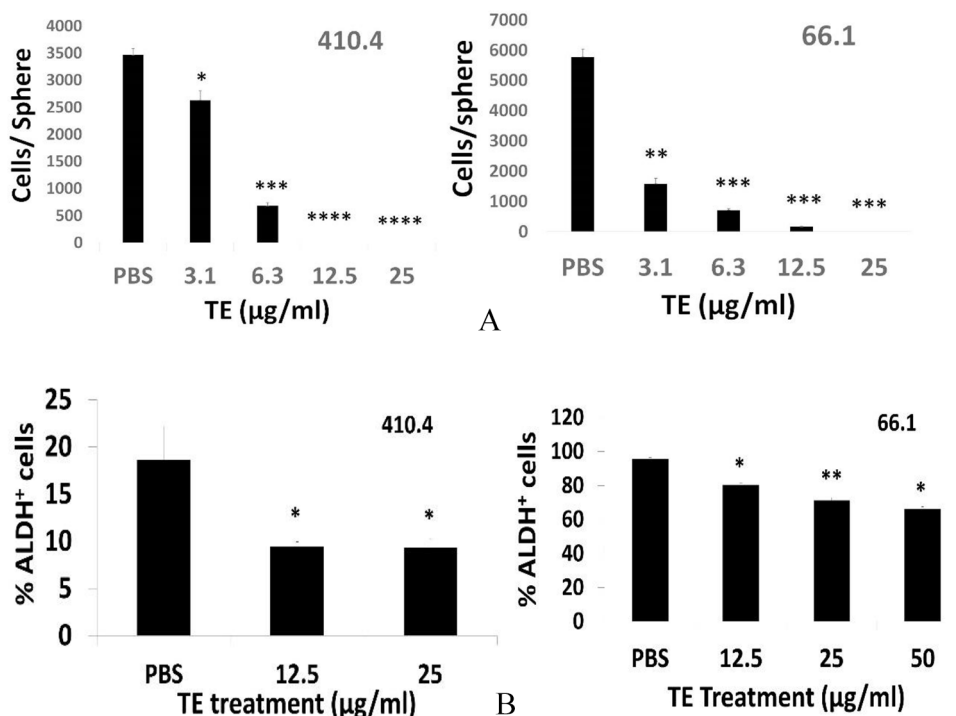
Figure 4. TE inhibits cancer stem cells. (A) 410.4 or 66.1 cells plated in low attachment conditions and primary tumorspheres allowed to form in the presence of TE or PBS control. On day 10, tumorspheres were dissociated, and size expressed as cells per sphere. *P* values: *P < .01; **P < .0002; ***P < .00005; ****P < .000007. (B) 410.4 tumorspheres treated with vehicle or TE, tumorspheres harvested (day 8), dissociated and fraction of ALDH1 + cells determined. *P < .06. Fraction of ALDH1 + cells in secondary 66.1-derived tumorspheres. *P < .004; **P < .002. PBS indicates phosphate-buffered saline; TE, taro extract.
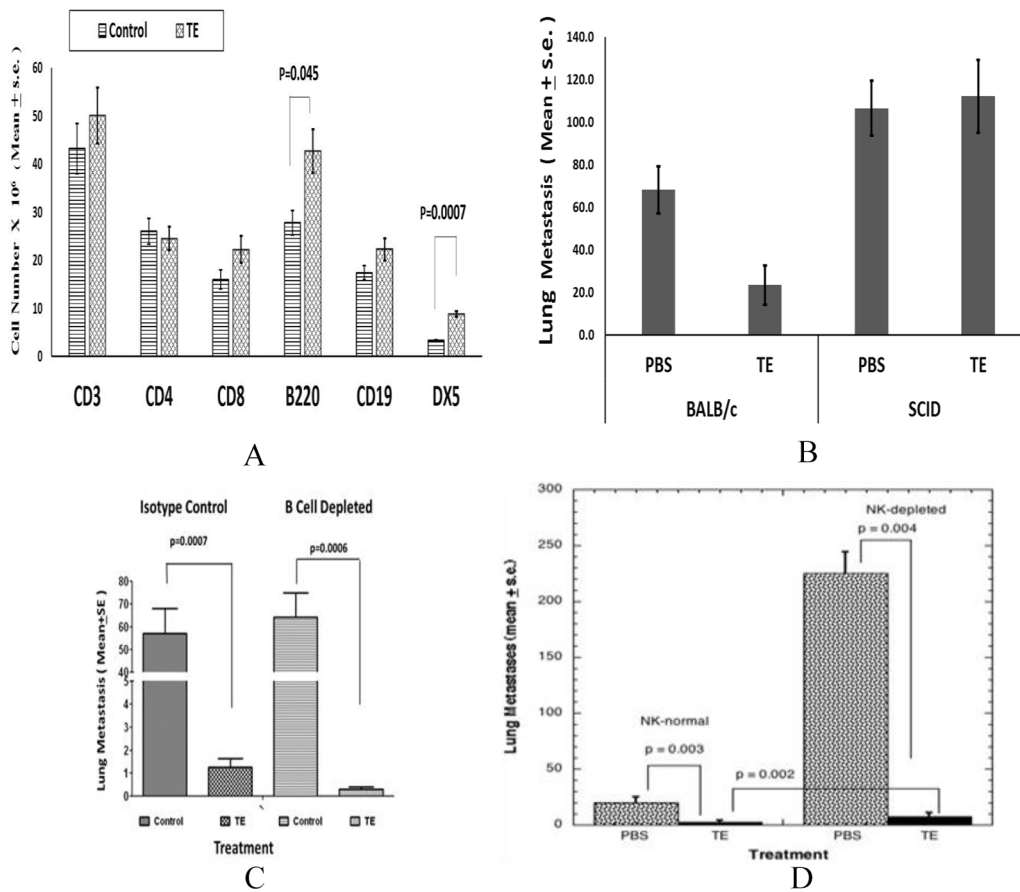
Figure 5. (A) Normal female Balb/cByJ mice treated with TE (400 µg/200 µL PBS) or vehicle for 4 days, spleens isolated and number of each cell type determined by flow cytometry. (B) Balb/cByJ or Balb/cSCID mice (5-6/group) treated with TE or PBS beginning on day 1 and continuing for 10 days. On day 4, mice injected with 1×10^5 line 66.1-luc tumor cells and on day + 19, lung metastases determined. PBS, Balb/cByJ versus TE, Balb/cByJ, $P = .05$. (C) On day 1, Balb/cByJ female mice (10/group) were treated with CD20 antibody or isotype control. On days 8 to 11, mice were treated with PBS or TE (400 µg/200 µL/day). On day 11, 1×10^5 of 66.1 cells injected IV. PBS or TE continued for an additional 6 days. On day 12, mice were again treated with either CD20 antibody or isotype control. Between days 14 and 21, mice were euthanized and lung metastases were enumerated. (D) On days + 1 to 10, Balb/cByJ female mice (10/group) were treated with PBS or TE (400 µg/200 µL/day). On days 3 and 7, mice were treated with asialo-GM1 antibody or normal rabbit serum. On day 4, 1×10^5 line 66.1 cells injected IV. On day 19, mice euthanized, and lung metastases were enumerated. PBS indicates phosphate-buffered saline; SCID, severe combined immune deficient; TE, taro extract.

peeled using an electric peeler (Starfrit 093209-006-BLCK Rotato Express, Quebec, Canada). The root was further cut into 1 cm pieces, mixed with standard phosphate-buffered saline (PBS) buffer (1:1 w:w) and ground in a food processor (Black & Decker quick easy food processor, CT) at high speed for 2 minutes to liquefy. After blending, the mix was centrifuged at 4000 r/min for 20 minutes. The collected supernatant was centrifuged at 15 000 r/min for 20 minutes. All centrifugation steps were carried out at 4°C. This method was employed for studies reported in Figures 6 and 7.

The extract was further fractioned into 3 molecular weight ranges via ultrafiltration: less than 10,000, between 10,000 and 30,000, and greater than 30,000. First, the supernatant was centrifuged through Amicon Ultra 10K Nominal molecular weight limit (NMWL) filter (Millipore Corp, MA) at 4,000 g for 45 minutes at 25°C. Based on previous research, the fraction less than 10,000 does not contain proteins of interest; thus, it was discarded.[3] Second, the size fraction greater than 10 kDa was centrifuged through 30,000 filter tube at 4,000 g for 45 minutes at 25°C. The fraction less than 30,000, that is, the cut between 10,000 and 30,000, and the fraction greater than the 30,000 filter cutoff were collected as concentrated stock TE for analysis. These concentrated stock solutions were further fractionated using SEC to obtain the final solution for testing.

To further purify the sample, 5 mL of a concentrated stock solution was directly loaded onto a HiPrep 16/60 Sephacryl S-200 HR column (GE Healthcare), connected to an AKTAFPLC system. The protein fractions were monitored using UV absorbance at 280 nm. The mobile phase buffer was 0.05 M sodium phosphate and 0.15 M sodium chloride with pH of 7.2 and flow rate of 0.5 mL/min. The column was calibrated with a gel filtration standard kit (Biorad #1511901, Hercules, CA), containing thyroglobulin, bovine γ-globulin, chicken ovalbumin, equine myoglobin, and vitamin B12, with m.w. of 670,000; 158,000; 44,000; 17,000, and 1,350 g/mol,
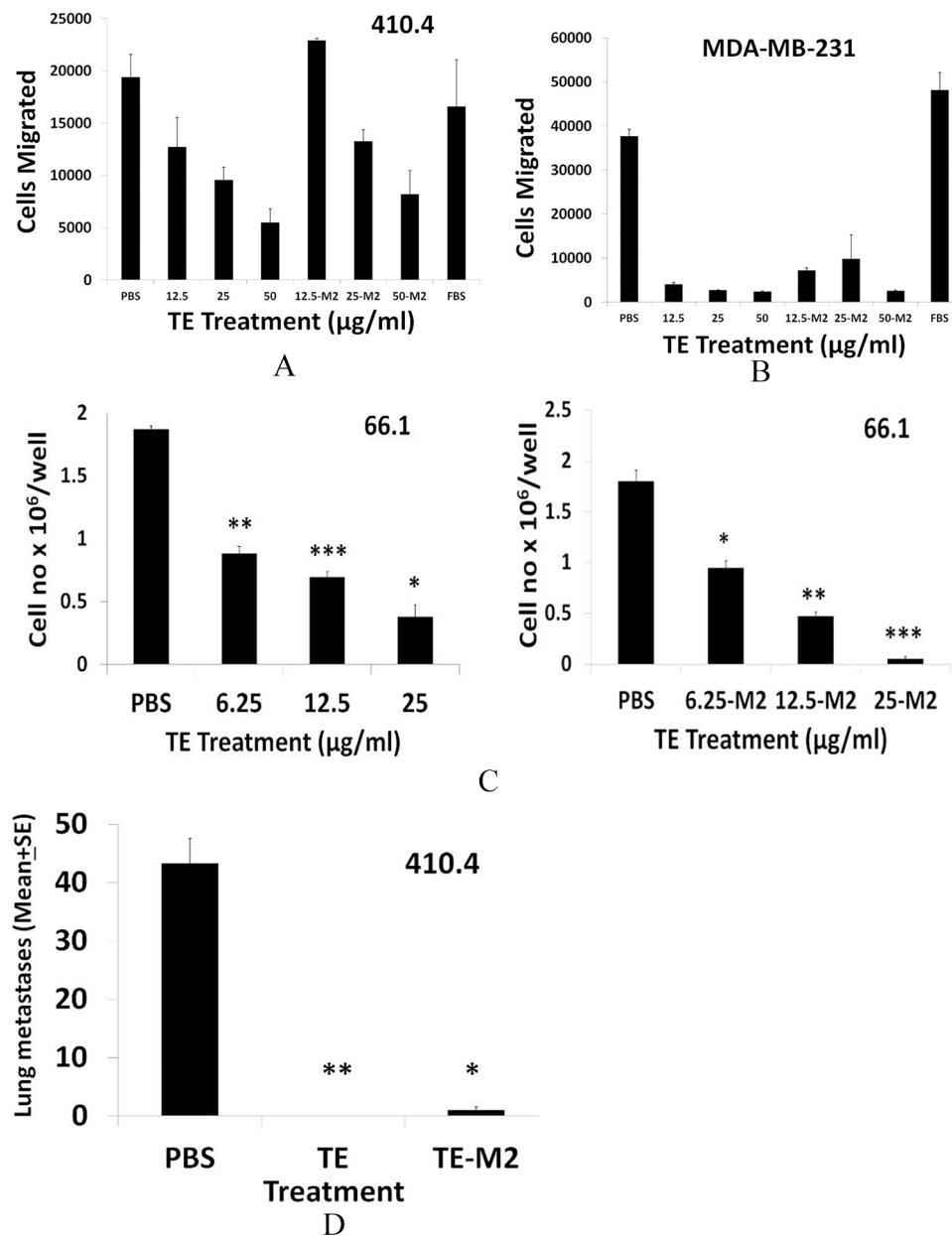
Figure 6. (A) The 410.4 or (B) MDA-MB-231 cells were resuspended in OPTI-MEM and placed in the upper well of Millicell tissue culture plates with inserts. PBS, TE, or TE-M2 at 12.5-50 μg/mL in OPTI-MEM containing 2% FBS was placed in the bottom chamber. Twenty hours later, cells in the lower chamber were stained with Calcein AM, dislodged using colorless trypsin and cell number estimated at Ex-485 and Emi-520 and plotted as average cells migrated. (C) The 1×10^4 of 66.1 cells plated in ultra-low attachment plates in triplicate. PBS, TE, or TE-M2 was added at time 0. On day 10, tumorspheres were harvested, dissociated and cell number/well was calculated. *$P < .003$; **$P < .001$; ***$P < .0001$. (D) Balb/cByJ female mice treated with PBS, TE, or TE-M2 (400 μg/day from days 1-10). On day + 4, mice were injected with 1.5×10^5 line 410.4 cells by IV route. On day + 20, mice were euthanized and surface lung tumors enumerated. *$P < .0006$; **$P < .00007$. FBS indicates fetal bovine serum; PBS, phosphate-buffered saline; TE, taro extract.

respectively. After initial analysis of the chromatograms, the samples were collected using a fraction collector. Using the > 30,000 filter solutions, the SEC fraction between 17,000 and 44,000 kDa was collected as TE-M2F1.

TE-M2F1 was spray dried using a Buchi B-290 spray dryer (BUCHI Corp., New Castle, DE) in open-loop mode using ambient air. The solution was pumped into the atomizer at a rate of 3 g/min. The inlet and outlet temperatures were 105°C and 56°C, respectively. The atomizing gas was set to 40 lbf/in². The spray dried powder was collected and stored at −20°C.

After rehydration with buffer, the isolated TE-M2F1 and Fraction 2 were analyzed using ultra performance liquid chromatography (UPLC) with ACQUITY UPCL H-class system with UV-C detection (Waters Corp., Milford, MA) using a 330A Jupiter C5 column (Phenomenex, Torrance, CA). The separation was done using gradient elution from 1% solvent A to 100% solvent B over 40 minutes at flow rate of 1 mL/min. Solvent A consisted of 0.1% trifluoroacetic acid (TFA) in water, solvent B consisted of 0.1% TFA in water: acetonitrile mixture 20:80. Detection as monitored at 250 nm.

Tumor cell lines

Murine mammary tumor cell lines (66.1, 66.1-luciferase, and 410.4) were maintained in DMEM (Dulbecco's Modified Eagle Medium) supplemented with 10% fetal bovine serum (FBS) (Gemini Bio-Products, Inc., Calabasas, CA, USA), 2 mM glutamine, penicillin (100 units/mL), streptomycin (100 μg/mL), and 0.1 mM nonessential amino acids in a 10% and 5% CO_2 humidified atmosphere, respectively. Human breast cancer cell line T47D was cultured in RPMI 1640 supplemented with 10%
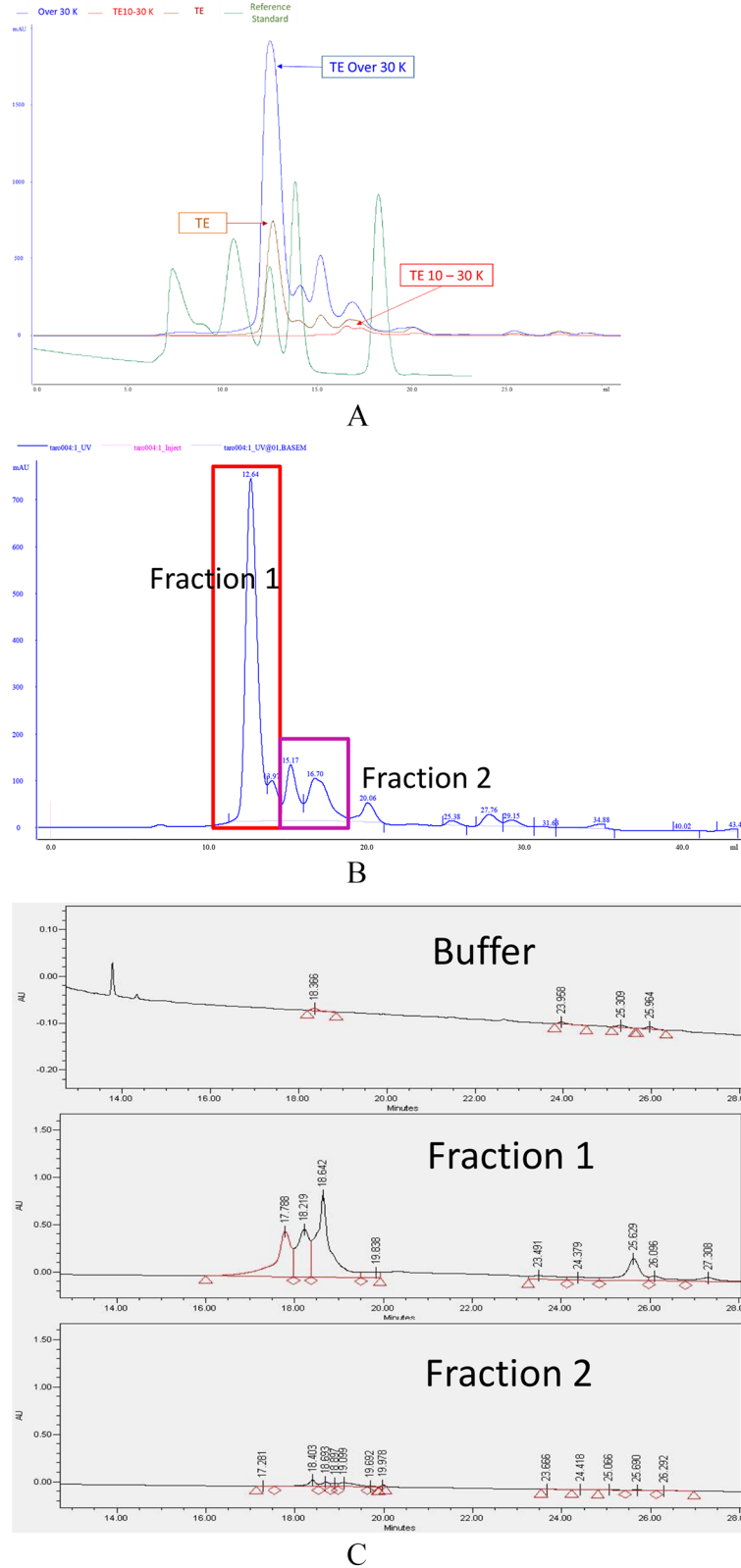

Figure 7. *(Continued)*

PBS

TE-M2-F1-25 µg/ml **TE-M2-F1- 50 µg/ml**

TE- 25 µg/ml **TE- 50 µg/ml**
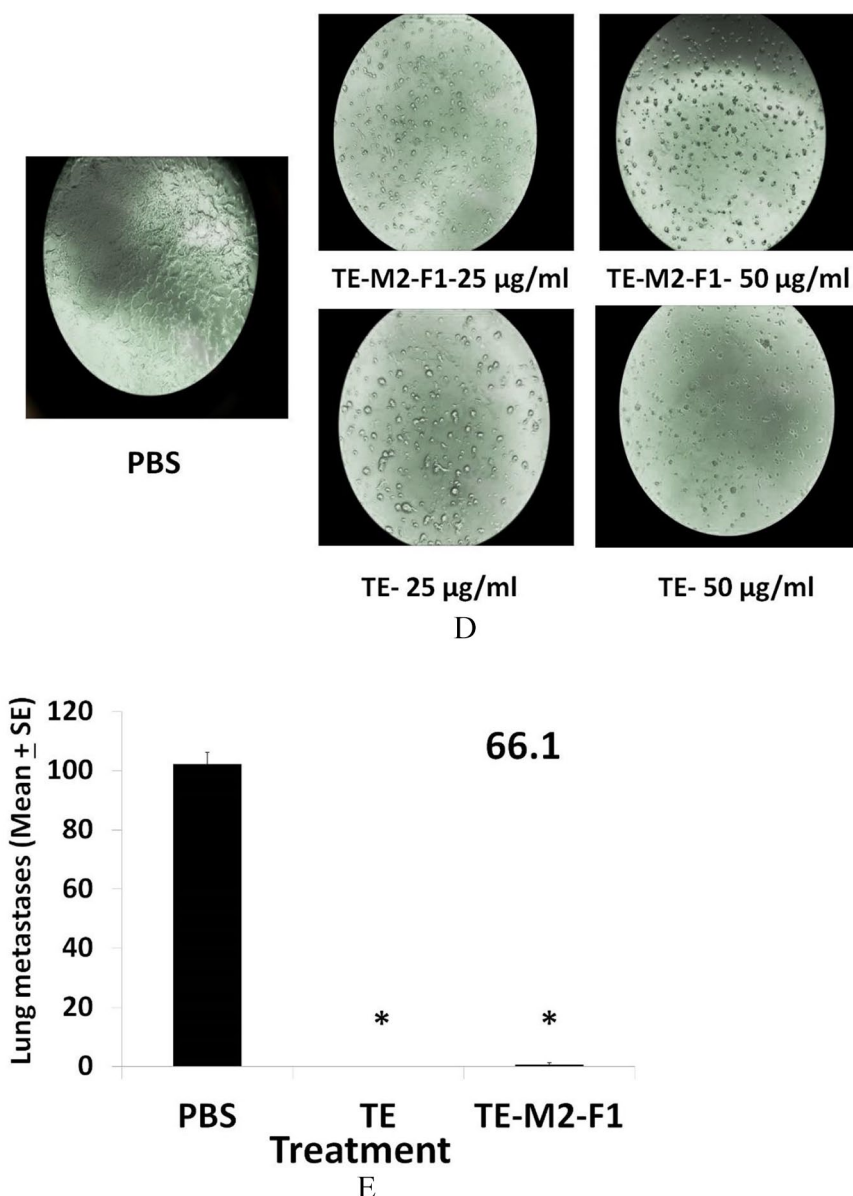
D

66.1

E

Figure 7. (A) Chromatography of TE (brown line), the 10 to 30 kD filter (red line) and the > 30 kD (blue line) fractions and a molecular weight standard (shown in green). The m.w. standards are described in "Methods" section. (B) An expanded view of the > 30 kD fraction with (C) a high resolution UPLC chromatogram of Fraction 1 and Fraction 2, from (B). (D) 66.1 cells grown in the presence of PBS, TE, or TE-M2F1 for 72 hours and morphology compared. (E) Balb/cByJ female mice treated with PBS, TE, or TE-M2F1 (200 µg/200 µL/day) on days 1 to 10. On day + 4, mice were injected with 1.5×10^5 line 66.1 tumor cells. On day + 19, mice were euthanized and surface tumor colonies enumerated. *$P < .0003$. PBS indicates phosphate-buffered saline; TE, taro extract; UPLC, ultra performance liquid chromatography.

FBS, penicillin, streptomycin, in a 5% CO_2 humidified atmosphere. The MDA-MB-231 and MDA-MB-468 cells were maintained in DMEM supplemented with 10% FBS, 2 mM glutamine, penicillin, streptomycin in a 10% CO_2 humidified atmosphere. Human breast cancer cell line BT549-GFP was maintained in high glucose DMEM supplemented with 10% FBS, 2 mM glutamine, antibiotics, and grown in a 10% CO_2 atmosphere. Ovarian cancer cell line NCI-ADR-RES-luc was maintained in DMEM containing 4.5 g/L glucose, 10% FBS, penicillin, streptomycin in a 5% CO_2 humidified atmosphere. Ovarian cell line OVCAR-3 was maintained in RPMI 1640 (Corning, Lowell, MA, USA), 20% FBS, penicillin and insulin

(0.01 mg/mL) in a 5% CO_2 humidified atmosphere. Murine cell lines have been maintained in the laboratory of AF for more than 30 years. Human cell lines were acquired from collaborators or ATCC. All cell lines have been verified within the last 5 years. For cell viability assays, cells were seeded in 24-well plates and PBS or TE was added at time 0. Seventy-two hours later, cell metabolic activity, as an indicator of cell growth, was determined by MTT assay following the manufacturer's instructions (Sigma Chem. Co., St. Louis, MO, USA). To facilitate the identification and comparison of sensitive versus resistant cell lines, data are plotted as percent inhibition relative to 0% inhibition in the control culture.

Metastasis assay

Either PBS or TE, TE-M2, or TE-M2F1 was delivered by intraperitoneal injection (IP) in a volume of 200 μL, into syngeneic Balb/cByJ female mice or Fox Chase SCID female mice on days 1 to 4. On day 4, 1-2 $\times$ 10^5 line 66.1 or 410.4 tumor cells were injected into the lateral tail vein. Treatment continued daily for an additional 6 days. Between days 14 and 21 post tumor cell injection, when control animals became moribund, mice were euthanized, and surface lung tumor colonies were counted under a dissecting microscope. For bioluminescent imaging, Balb/cByJ female mice were treated daily with TE (400 μg/200 μL) or PBS for 10 days. On day 4, 2 $\times$ 10^5 66.1-luc cells were injected into the lateral tail vein. Cells were detected by bioluminescent imaging (IVIS 200; Xenogen, Alameda, CA, USA) of anesthetized mice injected IP with 100 μL of 7.5 mg/mL D-luciferin (Perkin Elmer, Waltham, MA, USA) on days + 1, + 4, and + 15 relative to tumor cell injection. Bioluminescence from the regions of interest was defined manually and the data were expressed as photon flux (photons/s/cm^2/steradian) and analyzed by IVIS software. Euthanasia achieved by CO_2 asphyxiation followed by cervical dislocation.

Migration assay

Conducted as previously described in detail.[3] Briefly, tumor cells were resuspended in OPTI-MEM medium and placed in the upper well of Millicell tissue culture (24 well) plate well inserts, 8 or 12 μm (Millipore Ireland Ltd, Ireland). Fetal bovine serum (FBS, 2%) in OPTI-MEM containing no TE (control) or TE at 1 to 50 μg/mL final concentration, was placed in the bottom chamber. In some experiments, TE was also present in the upper chamber. Non-migrated cells removed under vacuum. Migration was assessed at 16 to 18 hours, as previously described. Results expressed as mean ± SE of triplicate wells.

Tumorsphere assay

Tumorsphere assays were performed as previously described in serum-free MammoCult medium (StemCell Technologies, Vancouver, BC, Canada).[9] Line 410.4 or 66.1 cells were plated in 24-well ultra-low attachment plates in triplicate (Corning, Lowell, MA, USA). The PBS or TE was added at the time of plating. About 8 to 10 days later, sphere counts were taken from each well. Spheres were dissociated using trypsin and cell number/sphere was calculated.

Breast CSC phenotyping

The Aldefluor assay was performed using Aldefluor kit (StemCell Technologies) following the company protocol. Fluorescence intensity was analyzed by FACSCanto II cytometer and data were analyzed with FlowJo software in the Flow Cytometry Shared Service of the UMGCCC.

Spleen cell phenotyping

Syngeneic Balb/cByJ female mice were treated IP with PBS or TE (400 μg/200 μL) on days 1 to 4. On day 5, mice were euthanized and spleens were harvested for phenotyping. Whole spleen cell suspensions were treated with RBC lysis buffer and washed twice with PBS. A 1 $\times$ 10^6 cell suspension was taken per tube and fluorescence conjugated antibodies (all from BD Pharmingen) or appropriate isotype control antibody to CD3+ (PE-Cy5, hamster anti-mouse CD3e), CD4+ (PE-Cy5 rat anti-mouse CD4), DX5 (PE-rat anti-mouse CD49b), B220 (PE-rat anti-mouse CD45R/B220), CD19+ (FITC-rat anti-mouse CD19), CD8+ (PE Cy5 rat anti-mouse CD8a) were added. After 1 hour, cells were fixed in paraformaldehyde (1%) and analyzed by FACScan analysis. Results are expressed as the percent of the total spleen cells positive for the individual marker.

B cell depletion

Syngeneic Balb/cByJ female mice were injected IP with either anti-mCD20 antibody (18B12, IgG2a isotype, 250 μg), or isotype control, generous gifts from Biogen (Cambridge, MA) on day 1. On days 8 to 11, PBS or TE (400 μg/200 μL) was administered IP. On day 11, 1 $\times$ 10^5 line 66.1 tumor cells were injected into the lateral tail vein. Treatment with PBS or TE continued (400 μg/200 μL) daily for an additional 6 days and isotype or antibody treatment was repeated on day 12. Between days 14 and 21 post tumor cell injection, when control animals became moribund, mice were euthanized, and surface lung tumor colonies were counted under a dissecting microscope.

Natural Killer cell depletion

Syngeneic Balb/cByJ female mice were treated with PBS or TE (400 μg/200 μL) by IP route on days 1 to 4. On day 4, 1 $\times$ 10^5 line 66.1 tumor cells were injected into the lateral tail vein, PBS or TE treatment continued for an additional 6 days. To deplete Natural Killer (NK) cells, some animals were treated with asialo GM1 antibody (Wako Bioproducts, Richmond, VA) (lyophilized antibody reconstituted in 1.0 mL distilled water, diluted 1:5 and 100 μL injected), 1 day prior to and 3 days after tumor cell injection. On day 19 post tumor cell injection, mice were euthanized, and surface lung tumor colonies were counted.

Statistical analysis

Data were summarized using descriptive statistics, means and standard errors, medians and ranges. Depending on the data distribution, the Student's *t*-test, or its non-parametric alternative, the Wilcoxon test, was used to compare distribution of metastases between treatment groups. All statistical tests were exact and done at the 2-sided .05 level of significance.

Results

The potent anti-metastatic activity of TE was reported previously.[3] This finding has now been replicated in 16 experiments totaling more than 200 mice, confirming that treatment of syngeneic Balb/cByJ female mice with TE (400 μg/200 μL/day, prepared by method 1) and hereafter referred to as TE, inhibits from 87% to 100% of lung metastases in 2 syngeneic models of TNBC (66.1; 410.4). Two representative experiments are shown (Figure 1A) in which 99% of 66.1 or 100% of 410.4 lung metastases were inhibited by TE. Bone marrow and brain are common sites of clinical breast cancer metastasis. Using bioluminescent imaging, we are now able to report that metastases to brain and bone marrow of 66.1-luc cells are also inhibited by TE (Figure 1B and C).

The TE efficacy could result from direct inhibitory effects on the malignant cells and/or by indirect mechanisms involving host immune responses. Moreover, the anti-cancer mechanism is not likely restricted to breast cancer. To continue to examine inhibitory effects on cell viability reported earlier,[3] we examined tumor cell-autonomous effects of TE on a larger panel of breast as well as ovarian cancer cell lines of either murine or human origin. Marked alteration in the tumor cell morphology was observed in the presence of TE, in some, but not all cell lines examined, with marked rounding up of treated cells and loss of cell/cell and cell/substrate contact (Figure 2A). The effect on morphology of 66.1 cells is representative of multiple responsive cell lines. The TE inhibited the viability of murine breast cancer cell lines 66.1, 410.4, human MDA-MB-231, and the human ovarian cancer cell lines NCI/ADR-RES-luc and OVCAR-3-luc (Figure 2B). Data are plotted as percent inhibition to compare the relative sensitivity of different cell lines to inhibition by TE. The inhibition observed in Figure 2B is not a universal response as human breast cancer cell lines MDA-MB-468 and T47D were not affected by TE as measured by this assay (Figure 2C). Note that in Panel 2C, data are plotted as % viable, because no statistically significant inhibition was observed. The ability of TE to affect tumor cell migration was examined next. The TE inhibited tumor cell migration of all 4 breast cancer cell lines examined (murine or human) (by 50%-80%) in a dose-dependent manner (Figure 3). Thus, TE has direct inhibitory activities against tumor cells as indicated by effects on cell morphology, growth, and migration.

To this point, we have largely confirmed our earlier studies using an expanded panel of human breast as well as ovarian cancer cell lines. We sought additional mechanisms that contribute to the anti-metastasis activity of TE. There is considerable data in support of the hypothesis that tumor-initiating cells are a select subset of tumor cells that share properties with normal tissue stem cells.[10] These cells retain pluripotency, are typically not highly proliferative but may, in cancer, represent the most aggressive, treatment-resistant populations. We therefore tested the new hypothesis that the marked anti-metastasis

efficacy of TE is accompanied by the ability to inhibit cancer cells with stem-like properties (*C*ancer *S*tem *C*ells). The effect of TE on functional properties of CSC (ability to form tumorspheres) and phenotypic indicators of stemness (aldehyde dehydrogenase activity) were assessed in 2 TNBC cell lines. Lines 410.4 and 66.1 each forms characteristic multi-cellular spheroids when grown under low attachment conditions in stem cell-supportive medium.[9] The addition of TE to mammosphere cultures of either cell line markedly reduced the number of large, mature tumorspheres, resulting in the appearance of many more, but much smaller diameter, multi-cellular structures that are too numerous to count accurately. When these spheres were harvested, dissociated and total cell number calculated, the total number of sphere-forming cells, derived from either 410.4 or 66.1, was decreased in the presence of TE in a dose-dependent manner (Figure 4A). High expression of aldehyde dehydrogenase 1 activity is an indicator of a breast CSC phenotype. As is commonly observed for independent cell lines, the percentage of enzyme positive cells varied by line. Treatment of 410.4 or 66.1 tumorspheres with TE significantly reduced the percentage of ALDH1 + tumor cells (Figure 4B).

Several groups report that exposure of normal mouse splenocytes to taro-derived proteins or treatment of normal mice with TEs leads to reversible enlargement of the spleen.[4-8] It was not known if this cell expansion was mechanistically related to the control of metastasis. We now report the characterization of spleen cell phenotypes in normal Balb/cByJ female mice treated with TE for 4 days. Spleen cell suspensions were prepared, RBC were lysed, and cells were identified with fluorescence conjugated antibodies or appropriate isotype control antibody to the following T lymphocyte markers: CD3, CD4, CD8; B cells were identified by B220 or CD19 expression, NK cells by DX5 expression. B220-positive B cell and NK cell populations were significantly increased in number in response to TE (Figure 5A). More modest changes in T lymphocyte subsets (CD3+; CD8+) were not statistically significant. Myeloid cells were also increased by 2-fold in TE-treated mice (not shown).

While several groups hypothesized that the changes in immune cell numbers in mice treated with Taro proteins represented a functional anti-tumor immune response, a mechanistic role for these responses has not been investigated. We sought to determine whether the changes in immune cell numbers are *mechanistically* related to the anti-metastatic activity of TE. The TE efficacy was compared in BALB/c/SCID mice lacking mature T and B cells to immune competent BALB/c/ByJ mice (Figure 5B). In the latter host, TE treatment resulted in a reduction in lung colonization from 68 ± 11 to 23 ± 9 average lung metastases. When the same experiment was carried out in BALB/c/SCID mice, with functional defects in both T and B cells, no reduction in lung tumor colonies was observed in TE-treated mice compared with control-treated mice (112 ± 17 vs 107 ± 13 lung metastases, respectively). A second, independent experiment led to the same conclusion;

that TE is no longer able to inhibit metastasis in immune-compromised BALB/c/SCID mice (data not shown).

To more clearly define the critical immune cell, we determined the effect of selective depletion of B or NK cell populations on TE efficacy. Mature B cells were depleted by treatment of mice with anti-murine CD20 antibody, resulting in depletion of 90% of B cells. As expected, treatment of mice with isotype control Ig did not compromise the ability of TE to control metastasis. The TE treatment resulted in marked reduction in lung metastases versus PBS-treated mice (1.25 ± 0.4 vs 57.1 ± 10.8 lung metastases, $P = .0007$, Figure 5C). Comparable TE efficacy was observed in mice depleted of mature B cells (0.3 ± 0.1 lung met vs 64.4 ± 10.5, $P = .0006$) indicating that B cells do not contribute to the mechanism of TE action.

Like B cells, NK cells were also increased in number in normal mice in response to TE. We determined TE efficacy in the setting of NK cell depletion. The TE inhibited 87% of lung metastases in NK-replete mice ($P = .003$, Figure 5D). Depletion of NK cells markedly increased the number of lung metastases in PBS-treated mice (225 ± 8) indicating that endogenous NK cells function to control tumor dissemination. Nevertheless, TE treatment in NK-depleted animals was still highly effective at reducing lung colonies in comparison with PBS-treated, NK-depleted mice (92% inhibition; $P = .004$) indicating that the major mechanism by which TE controls metastasis is likely to be independent of NK activity. As more lung metastases were observed in TE-treated, NK-depleted mice versus TE-treated, NK-replete mice ($P = .002$), a minor role for NK cells underlying the anti-metastatic activity of TE may be indicated. Taken together, these studies indicate that TE efficacy depends chiefly on functional T lymphocytes, but not B lymphocytes or NK cells.

An isolated fraction of TE was shown previously to retain the anti-metastatic activity of crude TE.[3] We sought to confirm these findings in an independent laboratory (SH) and to identify a scalable and GMP-adaptable method to isolate sufficient TE to support future clinical trials. We first confirmed that TE isolated using an updated method 2 (TE-M2) replicated the activity of TE prepared in the Fulton lab by the previously published method.[3] As an initial screen, the ability of TE-M2 versus TE to inhibit tumor cell migration was compared directly. As shown in Figure 6, TE independently isolated in 2 laboratories, that is, TE and TE-M2, confirmed the ability of TE to inhibit migration of either murine 410.4 (Figure 6A) or human MDA-MB-231 cells (Figure 6B). Likewise, either TE or TE-M2 was able to potently inhibit tumorsphere-forming ability of 66.1 cells in a dose-dependent manner with comparable potency (Figure 6C). Finally, the ability of TE-M2 to inhibit metastasis was compared with TE (Figure 6D). Like TE, TE-M2 potently inhibited metastasis.

The TE is comprised of a mixture of proteins but we knew that efficacy was not found in a fraction of <10 kDa.[3] The TE-M2 was separated by molecular weight into fractions <10,000; 10,000 to 30,000, and >30,000 by ultra-filtration. The SEC chromatograms show that in the 10 to 30 kDa fraction, there are only a few proteins close to the 10,000 cutoff (Figure 7A). We focused further studies on the >30 kDa fraction. An expanded view of this fraction is shown in Figure 7B. In Figure 7B, the region designated Fraction 1 contains the main peak and a smaller shoulder. This is followed by several smaller peaks in the region labeled Fraction 2. Figure 7A shows the m.w. standard run, which allowed for the m.w. estimation of these proteins. In Fraction 1, the proteins have a m.w. range of 30 to 44 kDa and for proteins in Fraction 2, the m.w. range is below 30 kDa. These 2 regions of the chromatogram were collected and reinjected into the UPLC (Figure 7C). The middle panel shows the Fraction 1 region is comprised of 3 main peaks at a retention time of 18.218 and 1 smaller peak at a retention time of 25.629 minutes. The lower panel of Figure 7C shows that Fraction 2 is comprised of several smaller peaks. Based on previous research by our group, the prediction that the active therapeutic moiety was contained in Fraction 1 (TE-M2F1) was tested. After multiple injections in SEC, we obtained sufficient protein to perform spray drying of these pooled samples that were then compared with TE by in vitro and in vivo assays. We determined that TE-M2F1, like TE, affects the morphology of 66.1 cells (Figure 7D) in which cells retract foot processes and round up. We compared the ability of TE-M2F1 versus TE to inhibit metastasis of line 66.1 cells (Figure 7E); comparable and potent anti-metastatic activity was observed for both. Thus, we have identified a reproducible method to isolate an anti-metastatic activity from the taro plant that is amenable to large-scale preparation needed for future clinical studies.

Discussion

The taro plant is a major dietary staple in much of the world. In addition, components of taro have anti-viral and insecticidal activities as well as purported medicinal properties. In an excellent recent review article,[5] Periera et al summarized much of what is currently understood about *C esculenta* biological activities, biochemistry, and potential therapeutic applications in multiple disease settings. Potential anti-tumor activities are beginning to emerge. Anti-cancer activity was first demonstrated by Brown et al[2] when a soluble extract of *cooked* taro was shown to inhibit proliferation of colon cancer cells in vitro. We first reported anti-cancer activity in vivo. A water-soluble extract of raw Taro (TE) potently inhibited breast tumor metastasis in 2 preclinical models of TNBC.[3] Fractionation and purification studies identified the active component of TE as a protein closely related to Tarin, taro lectin, and 12 kDa storage protein. Anti-metastatic activity of a water-soluble TE was subsequently confirmed by another laboratory[7] but that activity was ascribed to polysaccharides, so the relationship to TE is not clear. A liposomal nanoparticle containing the taro-derived protein, designated taro lectin, inhibited proliferation of MDA-MD-231 cells as well as human glioblastoma U87

MG cells.[11] The current study confirms our earlier identification of a potent anti-metastatic activity of TE. The new findings in the current report shed light on multiple tumor cell-autonomous as well as host immune response-dependent mechanisms of action. We now provide data that support both direct (anti-proliferative, anti-migratory, anti-CSC) and immune-based mechanisms by which TE inhibits metastasis.

Using a panel of human and murine breast cancer cells and human ovarian cancer cell lines, we showed, by MTT assay that viability of most, but not all cell lines was modestly inhibited by TE. More marked was the ability of TE to inhibit tumor cell migration. These data are confirmatory of our earlier report and are consistent with the more effective inhibition of tumor cell metastasis compared with inhibition of mammary gland-implanted tumors.[3]

Cancer relapse is driven by the appearance of treatment-resistant populations with heightened metastatic capacity. The CSC hypothesis states that a subpopulation of pluripotent cells with low proliferative capacity resists standard therapies and survives to repopulate the bulk tumor with more aggressive populations that ultimately result in disease relapse and mortality.[10] There is intense interest in identifying strategies to selectively inhibit CSC. We have shown previously that breast CSCs overexpress cyclooxygenase-2 and that the Cox-2 pathway contributes to breast CSC survival.[9] Furthermore, TE is a potent inhibitor of COX-2 gene expression.[3] Breast CSCs underlie treatment resistance and are closely linked to metastatic potential. The current study tested the new hypothesis that TE directly inhibits breast CSCs. We report, for the first time, that TE inhibits CSCs. The ability of breast cell lines to form 3-dimensional tumorspheres under low attachment conditions was inhibited by TE as was aldehyde dehydrogenase activity; both are indicators of functional CSCs.

In a series of studies, Pereira has characterized bioactive proteins isolated from water-soluble TEs.[5,6,12,13] They showed that a 12 kDa polypeptide, identified as tarin by mass spectrometry, was mitogenic to spleen B cells. They propose that the intact protein is a heterodimer of 47 kDa comprised of 2 non-identical polypeptides and acts as a lectin to bind with high affinity to mannose and complex N-glycans. Interestingly, some of these ligands are expressed on tumor cells, viruses, and in the gastrointestinal tract of some insects, which could underlie target specificity. For example, glycan 213 is part of the CA-125 glycoprotein antigen on epithelial ovarian cancers cells; glycan 212 is part of the gp120 glycoprotein of HIV-1. Glycan 465 is a Lewis^y-type tetrasaccharide acting as a cancer-associated antigen in colon, stomach, ovary, breast, pancreas, prostate, and lung.[14,15,16] Vajravijayan et al[17] carried out a structural biological analysis of a taro-derived lectin purified by ion exchange chromatography. That study identifies a 12 kDa, mannose binding, Galanthus nivalis-related lectin that forms β-prisms. Thus, there is considerable consensus regarding a 12 kDa protein producing B cell stimulation and anti-metastatic activity.

Both Pereira et al and we have observed that TE-treated mice experience an expansion of B lymphocytes in the spleen and bone marrow.[4,5,6] We extended that observation to show that NK cells are also increased in the spleen but neither CD3+, CD4+, nor CD8+ T cell numbers were significantly altered in response to TE. Others have argued that the B cell expansion may be potentially beneficial in some settings; however, in the cancer models employed here, the B cell response does not appear to contribute to the *mechanism* of metastasis inhibition. B cell depletion did not compromise the ability of TE to inhibit tumor dissemination. Conversely, the loss of efficacy in Balb/c/SCID mice that we demonstrated implicates T lymphocytes in the therapeutic mechanism. Park et al[7] reported that treatment of normal mice with a TE enhanced the ability of splenocytes isolated from these mice to lyse Yac-1 tumor cells, an NK-sensitive target cell. That finding is consistent with the increased number of NK cells we observed in TE-treated normal mice; however, we have now shown that the ability of TE to inhibit metastasis is largely intact in mice specifically depleted of NK cells. Thus, in the current model, we found no evidence that either the observed B cell or NK cell expansion contributes significantly to the anti-metastatic activity of TE. The mechanistic role of any immune effector cell in the study by Park et al[7] is difficult to evaluate as that study employed an allogeneic model of B16 melanoma (H-2b) transplanted across a major histocompatibility barrier to BALB/c (H-2d) mice. While some of the hematopoietic expansion does not appear to be mechanistically related to the anti-metastatic activity of TE, a recent paper by Merida et al[8] reveals a protective effect of Tarin on cyclophosphamide-induced leukopenia in mice. Thus, taro-derived proteins may have multiple actions that are potentially beneficial in the setting of malignancy independent of the tumor-inhibitory activity.

In this report, we have also identified a fraction (TE-M2F1) that replicates the anti-metastatic activity of TE. Isolation of TE-M2F1 by a combination of ultrafiltration, SEC, and spray-drying identifies a potential method that is GMP-compatible that can be scaled up to produce sufficient quantities for clinical evaluation.

Conclusions

In summary, the current study confirms that a water-soluble TE has a remarkable ability to inhibit tumor metastasis. We used 2 preclinical models of triple negative metastatic breast cancer which represents the most challenging subtype of human breast cancer for which few treatment options are available. We also showed anti-proliferative activity against ovarian cancer and, combined with our previous demonstration that prostate cancer cell lines are inhibited, suggests that TE could have broad efficacy against a number of histologies. Importantly, we report the novel demonstration that TE potently inhibits breast CSCs that are predicted to underlie therapy resistance and relapse. In other new findings, our studies demonstrate, for the first time, that, even though TE induces marked expansion of B lymphocytes as well as NK cells in the spleen, neither cell

appears to contribute to the mechanism by which TE controls tumor dissemination. In contrast, a role for T lymphocytes is suggested by the loss of efficacy in BALB/cSCID mice lacking mature T and B cells. The mechanisms underlying this observation continue to be investigated. These studies provide further support for the continued examination of biologically active components of *C esculenta* as potential new therapeutic entities and identify a method to isolate sufficient quantities under GMP conditions to conduct early phase clinical studies.

Acknowledgements

Author Contributions

NK, XM, SH, FW and AI designed and conducted experiments. NK, AF, RGR, DW, SH contributed to initial drafts of the manuscript. AF provided overall oversight of experimental design, and final manuscript.

ORCID iDs

Ahmed Ibrahim [iD] https://orcid.org/0000-0003-1513-1014
Amy M Fulton [iD] https://orcid.org/0000-0002-7657-9683
Stephen Hoag [iD] https://orcid.org/0000-0003-0657-6951

REFERENCES

1. Brown AC, Ibrahim SA, Song D. Poi history, uses, and role in health. In: Watson RR, Preedy V, eds. *Fruits, Vegetables, and Herbs: Bioactive Foods in Health Promotion*. Oxford, UK: Academic Press; 2016:331-342.
2. Brown AC, Reitzenstein JE, Liu J, Jadus MR. The anti-cancer effects of poi (*Colocasia esculenta*) on colonic adenocarcinoma cells in vitro. *Phytother Res*. 2005;19:767-771.
3. Kundu N, Campbell P, Hampton B, et al. Antimetastatic activity isolated from *Colocasia esculenta* (taro). *Anticancer Drugs*. 2012;23:200-211.
4. Pereira PR, Silva JT, Verícimo MA, Paschoalin VMF, Teixeira GAPB. Crude extract from taro (*Colocasia esculenta*) as a natural source of bioactive proteins able to stimulate haematopoietic cells in two murine models. *J Funct Foods*. 2015;18: 333-343.
5. Pereira PR, Correa A, Vericimo MA, Paschoalin VMF. Tarin, a potential immunomodulator and COX-inhibitor lectin found in taro (*Colocasia esculenta*). *Compr Rev Food Sci Food Saf*. 2018;17:878-891.
6. Pereira PR, Del Aguila EM, Vericimo MA, Zingali RB, Paschoalin VM, Silva JT. Purification and characterization of the lectin from taro (*Colocasia esculenta*) and its effect on mouse splenocyte proliferation in vitro and in vivo. *Protein J*. 2014;33:92-99.
7. Park HR, Lee HS, Cho SY, Kim YS, Shin KS. Anti-metastatic effect of polysaccharide isolated from *Colocasia esculenta* is exerted through immunostimulation. *Int J Mol Med*. 2013;31:361-368.
8. Merida LAD, Mattos EBA, Correa A, et al. Tarin stimulates granulocyte growth in bone marrow cell cultures and minimizes immunosuppression by cyclophosphamide in mice. *PLoS ONE*. 2018;12:e0206240.
9. Kundu N, Ma X, Kochel T, et al. Prostaglandin E receptor EP4 is a therapeutic target in breast cancer cells with stem-like properties. *Breast Cancer Res Treat*. 2014;143:19-31.
10. Lin L, Hutzen B, Lee HF, et al. Evaluation of STAT3 signaling in ALDH+ and ALDH+/CD44+/CD24- subpopulations of breast cancer cells. *PLoS ONE*. 2013;8:e82821.
11. Correa A, Vericimo MA, Dashevskiy A, Pereira PR, Paschoalin VMF. Liposomal taro lectin nanocapsules control human glioblastoma and mammary adenocarcinoma cell proliferation. *Molecules*. 2019;24:471.
12. Pereira PR, Winter HC, Vericimo MA, et al. Structural analysis and binding properties of isoforms of tarin, the GNA-related lectin from *Colocasia esculenta*. *Biochim Biophys Acta*. 2015;1854:20-30.
13. Pereira PR, Meagher JL, Winter HC, et al. High-resolution crystal structures of *Colocasia esculenta* tarin lectin. *Glycobiology*. 2017;27:50-56.
14. Zhao R, Liu X, Wang Y, et al. Integrated glycomic analysis of ovarian cancer side population cells. *Clin Proteomics*. 2016;13:32.
15. Mallard BW, Tiralongo J. Cancer stem cell marker glycosylation: nature, function and significance. *Glycoconj J*. 2017;34:441-452.
16. Barkeer S, Chugh S, Batra SK, Ponnusamy MP. Glycosylation of cancer stem cells: function in stemness, tumorigenesis and metastasis. *Neoplasia*. 2018;20:813-825.
17. Vajravijayan S, Pletnev S, Pletnev VZ, Nandhagopal N, Gunasekaran K. Structural analysis of β-prism lectin from *Colocasia esculenta* (L.) S chott. *Int J Biol Macromol*. 2016;91:518-523.